

# Study of the working process of a dual-fuel hydrogen engine

*Andrey Kuleshov*<sup>1\*</sup>, *Alexey Kuleshov*<sup>1</sup>, *Vladimir Markov*<sup>1</sup>, *Fedor Karpets*<sup>1</sup>, *Venera Yumagulova*<sup>2</sup>, and *Aidar Nurullin*<sup>2</sup>

<sup>1</sup>Bauman Moscow State Technical University, Moscow, Russia

<sup>2</sup>Kazan Federal University, 18 Kremlin Street, Kazan, Russia

**Abstract.** The relevance of the article is due to the need to replace petroleum fuels with motor fuels obtained from alternative raw materials. Hydrogen is considered as a promising alternative fuel. The use of hydrogen as a motor fuel makes it possible to solve the problem of a cardinal reduction in carbon dioxide emissions into the atmosphere. Using the DIESEL-RK software package, computational studies of the effect of hydrogen supply on the working process of the gas-diesel engine D-245 were carried out. The diesel cycle of the engine and its gas-diesel cycle were calculated with hydrogen supplies equal to 5, 10, 20, 40, 60 and 80% (taking into account the difference in the heat of combustion of the studied fuels). The maximum effective efficiency of a diesel engine is achieved when 40% hydrogen is supplied to the combustion chamber. In this case, compared to operation only on petroleum diesel fuel, the effective efficiency of the diesel engine increased by 7%.

## 1 Introduction

Growing environmental problems and the gradual transition from fossil energy resources to alternative energy sources caused by these problems lead to a change in the structure of consumption of primary energy resources. With regard to transport power plants, the priority is the use of carbon-free motor fuels, which, first of all, include hydrogen [1–4]. Its wider application in internal combustion engines (ICE) will reduce the toxicity of exhaust gases (EG) and the emission of the main greenhouse gas, carbon dioxide, into the atmosphere.

The analysis performed confirms the prospects of using hydrogen as a motor fuel. The accumulated scientific and technical experience in using hydrogen as a fuel for internal combustion engines, as well as well-known research and development, show that hydrogen and hydrogen-containing gases are quite compatible with the existing basic design of a piston internal combustion engine [5–7]. At the same time, the use of hydrogen as a fuel for internal combustion engines is complicated by the existence of a number of problems due to its specific properties as a motor fuel.

When hydrogen is burned, the combustion process and the detonation phenomenon in the engine differ significantly from the combustion of hydrocarbon fuels. A very short ignition

---

\* Corresponding author: [askuleshov@mail.ru](mailto:askuleshov@mail.ru)

delay period for a stoichiometric and near-stoichiometric hydrogen-air mixture and a high combustion rate create problems of “hard” combustion, detonation, and backfires in the engine intake tract [8–10]. These features of the use of hydrogen as a motor fuel are due to significant differences in the physicochemical properties of hydrogen and petroleum fuels (Table 1).

**Table 1.** Properties of hydrogen, propane, gasoline and diesel fuel.

Properties	Hydrogen	Propane	Automobile gasoline	Diesel fuel summer
Composition formula	H <sub>2</sub>	C <sub>3</sub> H <sub>8</sub>	C <sub>8</sub> H <sub>17</sub>	C <sub>12</sub> H <sub>26</sub>
Molecular mass	2.02	44.09	114	172
Boiling point at p = 0.1 MPa, °C	-252.8	-42.0	40-200	180-360
Density at t=20° C and p = 0.1 MPa, kg/m <sup>3</sup>	0.090	2.02	720-750	800-850
Net calorific value: MJ/kg MJ/m <sup>3</sup>	119.9 10.8	46.4 91.3	44.0 -	42.5 -
The amount of air required for fuel combustion: m <sup>3</sup> / m <sup>3</sup> kg/kg	2.38 34.5	23.8 15.7	- 14.7	- 14.3
Limits of ignition in a stoichiometric mixture with air (by volume of vapors),%	4.0-74.2	2.3-9.5	1.6-6.0	-
Limits of ignition of a combustible mixture according to the coefficient of excess air*	0.32/8.70*	0.40/1.70*	0.65/1.10**	0.82/1.05*
Self-ignition temperature in the diesel combustion chamber, °C	510-590	440-480	350-400	250-300
Cetane number	About 1	16	8-15	45-55
Flame propagation speed in mixtures with air at various coefficients of excess air, m/s	1.6-2.6	0.40-0.45	0.37-0.43	0.35-0.40
Octane number according to the motor method ONE, units	70	100	80-100	-

Note: for motor gasoline and diesel fuel, indicators are given for fuels of medium composition; \* - lower limit/upper limit.

It should be noted that the rate of pressure increase in the combustion chamber (CC) of a hydrogen engine operating on stoichiometric and close to it mixtures is approximately three times higher compared to the combustion of gasoline-air mixtures. But when switching to lean mixtures of hydrogen with air, the rate of their combustion is significantly reduced, which ensures the normal operation of the engine [11, 12]. The leanness of the fuel mixture is achieved by increasing the excess air ratio, for example, in the range from 1 to 2.

Hydrogen is considered an environmentally friendly fuel. Since hydrogen fuel does not contain carbon, the composition of its combustion products theoretically should not contain carbon monoxide CO, light unburned hydrocarbons CH<sub>x</sub>, soot (carbon C) and carbon dioxide CO<sub>2</sub>. The source for emissions of these toxic exhaust gases is only the burning motor oil used

by the engine. However, these emissions are very small. Hydrogen is, in fact, the only fuel whose use can almost completely eliminate the release of carbon dioxide into the atmosphere, which enters the atmosphere in large quantities. And the combustion of carbon fuels results in annual emissions of carbon dioxide into the atmosphere exceeding 32 Gt. The product of combustion (oxidation) of hydrogen is water  $H_2O$  - complete hydrogen oxide. But at the same time, the combustion of hydrogen in the internal combustion engine is accompanied by a significant emission of nitrogen oxides  $NO_x$ , which is caused by the high combustion temperature of the working mixture and the intense oxidation of nitrogen contained in the air. But at the same time, ways to reduce emissions of this most significant gaseous toxic component of the exhaust gas are known. Of these, diesel engines are implemented: work with increased excess air ratios, charge air cooling, control of the fuel injection advance angle (FIAA), organization of exhaust gas recirculation, an increase in the vapor content in the working mixture, measures aimed at deforcing the engine (reducing the compression ratio, etc.). As a result, when hydrogen is burned in an internal combustion engine, it is possible to drastically reduce emissions of soot, CO,  $CH_x$ , and  $CO_2$  [13, 14, 15].

Different organization of the hydrogen engine operation is possible. Effective ignition of hydrogen in the combustion chamber can be ensured by supplying an ignition dose of petroleum diesel fuel to the cylinders [16, 17, 18]. The ignition of hydrogen from the heat of combustion of pilot diesel fuel provides the required ignition energy, especially in unforced modes, characterized by a lower temperature of the working mixture. This provides the simplest and most efficient way to organize the working process of a hydrogen engine. Such an organization of the working process makes it possible to solve the problem of hydrogen ignition and its combustion with acceptable combustion dynamics and improved exhaust gas toxicity. But this raises the problem of optimizing the ratio of the supply of oil diesel fuel and hydrogen. The aim of the study is a computational study of the effect of the amount of hydrogen supplied to the combustion chamber of such a gas-diesel engine on its environmental and performance indicators. This study was carried out by calculation using the DIESEL-RK software package (PC), developed at the Moscow State Technical University. N.E. Bauman by Professor A.S. Kuleshov and designed for thermodynamic calculation and optimization of ICE working processes [17, 18, 19].

## 2 Object of study

As an object of study, a diesel engine of the D-245 type (4 N 11/12.5) with an initial power of  $N_e = 84$  kW at a crankshaft speed of  $n = 2400$   $\text{min}^{-1}$  was chosen. This turbocharged engine (without charge air cooling) has a compression ratio of  $\varepsilon = 15$ , a cast-iron cylinder head and an aluminum piston with a deep combustion chamber of the TsNIDI type (Central Diesel Research Institute), Figure 1.

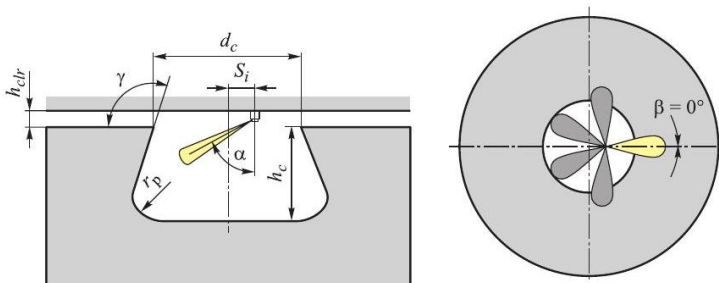


**Fig. 1.** The shape and dimensions of the CC of the D-245 engine: CC depth  $h_c = 28.6$  mm; external diameter of the CC  $d_c = 38$  mm; the angle of inclination of the generatrix of the CC wall to the plane (bottom) of the piston  $\gamma = 120^\circ$ ; rounding radius on the periphery  $r_p = 9$  mm; over-piston clearance

$h_{clr}=1$  mm; displacement of the nozzle axis relative to the axis of the cylinder  $s_i = 10$  mm; angle of inclination of the fuel jet axis relative to the atomizer axis  $\alpha$  (Table 3); the angular arrangement of the fuel jets relative to the atomizer pin  $\beta$  (Table 3).

The parameters of the diesel injector nozzle type D-245 are given in Table 2.

**Table 2.** Parameters of the spray nozzle diesel D-245.

Spray hole diameter $d_r$ , mm	Number of spray holes $i_r$	Maximum stroke of the needle $h_{nmax}$ , mm	Total effective area of atomizer assembly $\mu_{pf}$ , mm <sup>2</sup>
0.34	5	0.32	0.270

Note: the values of  $\mu_{pf}$  are given at the maximum lift of the nozzle needle  $h_{nmax} = 0.32$  mm;  $h_i$  and  $\mu_{pf}$  values are indicated average for a set of atomizers.

**Table 3.** The location of the spray holes of the diesel nozzle D-245.

Hole No.	Hole inclination angle relative to the atomizer axis $\alpha$ , deg	Angular location of the hole relative to the pin $\beta$ , deg
1	48.5	0
2	61.3	94.5
3	72.0	153.2
4	72.0	-153.2
5	61.3	-94.6

When calculating in DIESEL-RK, the standard diesel fuel injection system (DF – Figure 2, a) was taken for the fuel system "A". Due to the fact that the engine under consideration has practically no valve overlap, a hydrogen supply scheme was adopted with gas supply to the intake manifold. The hydrogen supply system is designated as system "B" (Figure 2b). The pressure of hydrogen in the line for its supply to the valve channels was set 1 bar higher than the boost pressure. In this case, the maximum gas flow rate is calculated based on the geometry of the flow part of the valve and the pressure drop in it. The shape of the characteristic of hydrogen supply from the angle of rotation of the crankshaft (p.k.v.) is adopted as trapezoidal. The start of gas supply is accepted - 300° p.k.v. to top dead center (TDC), cyclic supply of oil diesel fuel and hydrogen are presented in Table 4.

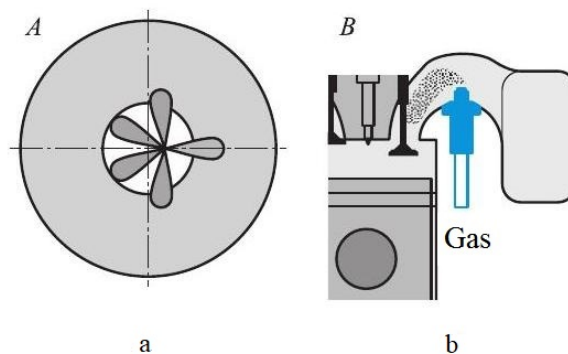


**Fig. 2.** The system for supplying oil diesel fuel to the cylinder of the D-245 gas diesel engine, which forms jets of atomized fuel (a), and the system for supplying hydrogen to the engine intake system (b).

Thus, it is assumed in the work that the supply of oil diesel fuel is carried out by a standard fuel system, and the supply of hydrogen in the gas phase is carried out to the intake system after the turbocharger. Cyclic supply of diesel fuel  $m_{DF}$  and hydrogen  $m_{Gas}$  for the studied modes are calculated taking into account the calorific value of diesel fuel and hydrogen and are presented in Table 4. The characteristics of the injection of oil diesel fuel are shown in Figure 3.

**Table 4.** Ratios of diesel fuel and hydrogen (gas) calculated for different cycles of engine operation.

Mode	No 1	No 2	No 3	No 4	No 5	No 6	No 7
Share of hydrogen, %	0	5	10	20	40	60	80
Share of diesel fuel, %	100	95	90	80	60	40	20
Hu <sub>df</sub> , MJ/kg	42.5	42.5	42.5	42.5	42.5	42.5	42.5
Hu <sub>gas</sub> , MJ/kg	120	120	120	120	120	120	120
Total fuel energy, kJ	2.809	2.809	2.809	2.809	2.809	2.809	2.809
$m_{DF}$ , g	0.0661	0.0628	0.0595	0.0529	0.0397	0.0264	0.0132
$m_{Gas}$ , g	0	0.00117	0.00234	0.00468	0.00936	0.01405	0.01873

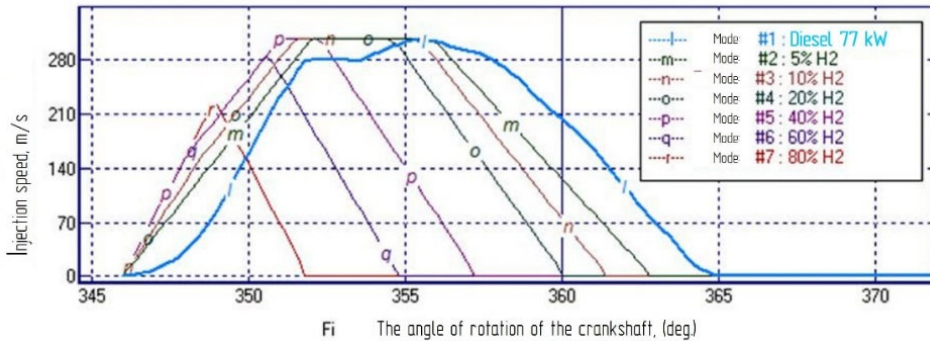


**Fig. 3.** Characteristics of diesel fuel injection in different modes with different cyclic hydrogen supply: *l* - calculation 1: 100% diesel fuel; *m* - calculation 2: 95% DF and 5% H<sub>2</sub>; *n* - calculation 3: 90% DF and 10% H<sub>2</sub>; *o* - calculation 4: 80% DF and 20% H<sub>2</sub>; *p* - calculation 5: 60% DF and 40% H<sub>2</sub>; *q* - calculation 6: 40% DF and 60% H<sub>2</sub>; *r* - calculation 7: 20% DF and 80% H<sub>2</sub>.

Since a significant increase in maximum pressures and combustion temperatures is noted with partial replacement of oil diesel fuel with hydrogen, even while maintaining the total calorific value of the fuels used, when this diesel engine is switched to dual-fuel operation (oil diesel fuel and hydrogen), the initial compression ratio  $\epsilon=15$  is reduced to  $\epsilon=8$ . FIAA is reduced from  $\theta=14^\circ$  r.a.c. up to TDC up to  $\theta=5^\circ$  p.c.v. to TDC. In addition, the diesel engine was derated to a speed of  $n=2200 \text{ min}^{-1}$  and, accordingly, to  $N_e=77 \text{ kW}$ . The share of hydrogen supplied to the combustion chamber in the total fuel supply is set at 5, 10, 20, 40, 60 and 80% (taking into account the difference in the combustion heat of diesel fuel and hydrogen).

### 3 Mathematical models used in computational studies of the working process of a gas-diesel engine

The PC DIESEL-RK implements modern mathematical models that allow simulating the working process of internal combustion engines, including multi-fuel engines. Such mathematical models of the PC DIESEL-RK include the following: a multi-zone model of mixture formation and combustion processes in a diesel engine, a 3-zone model of combustion in a gas diesel engine, several heat transfer models, a one-dimensional gas exchange model, a model of a two-stage turbocharging with charge air cooling, a model for calculating the emission of oxides nitrogen  $\text{NO}_x$  using a detailed kinetic mechanism, a model for calculating the emission of soot and particulate matter, a model for accounting for the exhaust gas recirculation system, etc. [17-19].

To calculate mixture formation and combustion in diesel engines, the RK-model is used, which is based on the calculation method proposed by Professor N.F. Razleytsev and further modified by Professor A.S. Kuleshov. The RC model takes into account the features of injection, including multiphase injection, the fineness of fuel atomization, the orientation of the jets in the volume of the combustion chamber, and the dynamics of the development of fuel jets.

The multizone model of mixture formation and combustion of a diesel jet is described in detail in [17–19]. The three-zone model of gas combustion in gas diesel used in this work is a new development. When using the three-zone model, the volume of the cylinder is divided into three characteristic zones (Figure 4):

- Jet zone before the end of injection: the volume occupied by developing and burning pilot (diesel) fuel jets.
- Jet zone during its advanced combustion: the remaining volume of the cylinder (excluding jet zones), in which the combustion of a homogeneous mixture of air, residual combustion products of diesel fuel and hydrogen takes place.
- Gas combustion activation zone, in which the working fluid is heated to a state, as a result of which stable combustion begins in the main zone. Below is a description of the basic principles for calculating the parameters of each of the three characteristic zones.

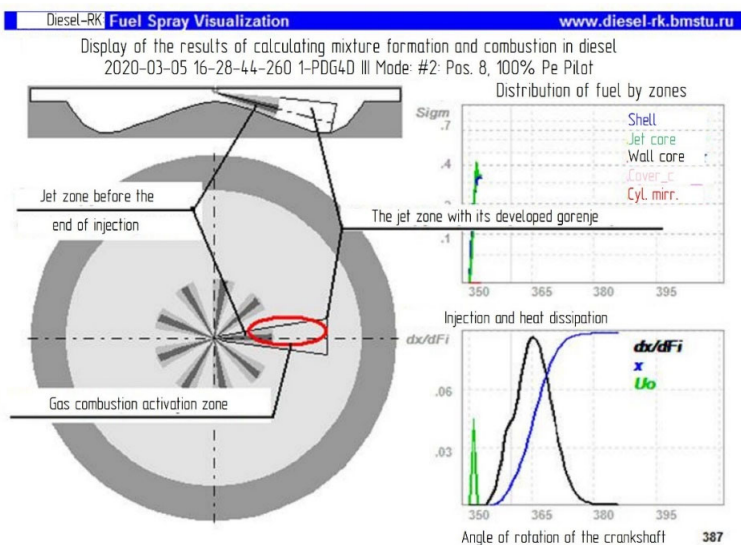


**Fig. 4.** Scheme of a three-zone model of gas combustion in a gas diesel engine, obtained using the Diesel-RK PC.

The jet zone before the end of injection has a conical shape and a variable volume calculated step by step through the geometry of the developing diesel jet. The geometry of the ignition jet and the rate of combustion (heat release) of diesel fuel in it are calculated within the framework of the RK model implemented in the DIESEL-RK program. The self-ignition delay period of diesel fuel  $\tau_{ign}$  is estimated by the modified formula (1) by A.I. Tolstov or by stepwise accumulation of the Livengood - Wu integral [19] - formula (3) with the definition of the instantaneous ignition delay  $\tau_{iT} = f(p, T, \alpha, BGF)$  as a function of pressure  $p$  and temperature  $T$  of the working mixture in the combustor, air excess coefficient  $\alpha$  and mass fraction of combustion products BGF (BurntGasFraction) by calculating the detailed chemical kinetics of preflame reactions in the CHEMKIN program.

In the latter case, the assumption  $\alpha=1$  is used for DF, since it is assumed that the reactions proceed most rapidly in the stoichiometric zone around the evaporating droplets. If before the flash all the droplets in the jet have time to completely evaporate, then the excess air coefficient  $\alpha$  after that is taken equal to the average value over the cylinder. In this study, the ignition delay calculation was carried out based on the value of the Livengood - Wu integral.

The kinetic mechanism LLNL-MI-536391 (n-heptanemechanismver. 3.1 2012-03-30) [20] is used as data for calculation in CHEMKIN, which, with the traditional organization of the working process in a diesel engine, gives a result close to the formula of A.I. Tolstov:

$$\tau_{ign} = 3.8 \cdot 10^{-6} (1 - 1.6 \cdot 10^{-4} n) \left( \frac{T}{p} \right)^m \exp\left( \frac{E_a}{8.312T} \right) C_c C_T, \quad (1)$$

where the exponent is defined as  $m = 0.64 - 0.035 p$  or approximately  $m = 0.5$ ;  $T$  – temperature, K;  $p$  – pressure, MPa;  $n$  – frequency of rotation of the crankshaft, min<sup>-1</sup>;  $E_a = 22.3$  kJ/mol – conditional activation energy of preflame reactions;  $C_c$  – coefficient taking into account the concentration of residual gases in the combustion products;  $C_T$  is a coefficient that takes into account the temperature dynamics during the delay period [21].

The jet of oil diesel fuel is injected very quickly and before its intense combustion (when the share of the released heat from the combustion of diesel fuel approaches the value  $\chi \approx 0.5$ ), it manages to occupy a rather large volume of the combustion chamber. The simplified Kuo formula [21] is used to extrapolate the jet range after the end of injection. The jet opening angle is estimated according to the criterion equations of A.S. Lyshevsky [19], which takes into account the properties of the fuel, injection pressure, diameter of the spray holes, and environmental parameters. Due to the intensification of mixing processes during combustion, the volume of the zone of the burning jet of diesel fuel exceeds the volume of the cone of the non-burning jet. The degree of increase in the volume of the jet is calculated by an empirical equation that takes into account the volume of the entire CS and the injection pressure. The temperature in the combustion zone of diesel fuel is calculated from the system of equations for the balance of mass, energy, concentration, and state [19], taking into account the burnout of hydrogen in the jet zone. It is assumed that hydrogen is homogeneously distributed in the charge of the cylinder and the mass of hydrogen that burns out in the jet zone is determined by the fraction of the jet volume in the volume of the entire cylinder. An analysis of the published experimental data shows that hydrogen in the jet zone burns out fairly quickly. To calculate the heat release rate of this gas, one can use the approximation of heat release  $x$  according to I.I. Vibe

$$x = 1 - \exp\left[ -6.908 \left( \frac{\phi}{\phi_z} \right)^{m_p+1} \right],$$

where  $m_p$  is the index of diffusion combustion;  $\phi_z$  is the duration of combustion, °r.c.v.;  $\phi$  is the current angle of rotation of the crankshaft (the beginning of combustion corresponds to  $\phi = 0$ ).

The jet zone during its developed combustion contains a homogeneous mixture of air, diesel fuel droplets, hydrogen and residual gases. The parameters in it are calculated using the same system of mass, energy, concentration, and state balance equations [19]. The heat release rate in this zone is calculated using the approximation by I.I. Vibe for the cycle mass of hydrogen minus the mass of the burn-out in the ignition jet zone. The combustion index for this zone is assumed to be constant  $m \cdot v \cdot m_z = 1$ . The duration of combustion  $\phi_{z.mz}$  in the main zone strongly depends on the gas excess air coefficient  $\alpha_{gas}$  and the temperature at the moment of starting the pilot fuel supply  $T_n$ . By analyzing the experimental data of different authors [22, 23, 24], we managed to obtain the empirical equation (2):

$$\phi_{z.mz} = \left[ 22.961 \cdot \ln(\alpha_{gas}) + \frac{6.5985}{\alpha_{gas}} - 0.18823 \cdot \alpha_{gas} \right] \cdot (1.4517 - 0.0007 \cdot T_n). \quad (2)$$

To estimate the moment of the beginning of hydrogen combustion in the main zone, a special zone of activation of gas combustion is allocated in the cylinder.

The gas combustion activation zone (Figure 4) has a constant volume located inside the zone of the oil diesel fuel jet and approximately equal to  $0.01 D_{cyl}^3$ . A proportionality factor of 0.01 serves to identify the mathematical model of hydrogen ignition in the main zone. If the volume of the oil jet zone is less than the volume of the activation zone, then the missing part of the activation volume is taken from the main zone. The temperature and composition of the mixture in the activation zone are calculated according to the additivity equations, which include temperatures, heat capacities, volumes and densities of the main zone and the ignition jet zone. Thus, the larger the activation zone, the slower the temperature rises in it, the later combustion starts in the main zone. The moment of ignition of hydrogen in the main zone can be estimated by reaching the predetermined temperature  $T_{activ} \sim 1100$  K in the activation zone, or by accumulating the Livengood-Wu(LW) integral of expression (3) over the current parameters of the activation zone. It is believed that ignition occurs when LW becomes equal to 1.

$$LW = \int_0^{\tau_i} \frac{d\tau}{\tau_{iT}}, \quad (3)$$

where  $d\tau$  is the calculated time step,  $c$ ;  $\tau_i$  is the autoignition delay period,  $c$ ;  $\tau_{iT}$  is the theoretical autoignition delay period (depending on the instantaneous values of the gas parameters in the activation zone:  $p$ ,  $T_{act}$ ,  $\alpha_{act}$ ,  $BG_{Fact}$ ),  $c$ . At each computational step,  $\tau_{iT}$  is determined by calculating the detailed chemical kinetics of preflame reactions using the CHEMKIN program. For hydrogen-air mixtures, the LLNL\_v1\_ab mechanism is used [25]. As soon as the fulfillment of the hydrogen ignition condition is registered in the activation zone, the heat release from gas combustion in the main zone is immediately taken into account. In the process of hydrogen burnout, the main zone loses volume and mass of the working fluid: the reacted mixture is transferred from this zone to the zone of combustion products, which grows from the initial zone of the pilot jet. The combustion calculation process takes into account the effect of expansion of the combustion zone and "compression" of the main zone (unburned charge) by iterative refinement of the increase in the volume of the zones to achieve equality of pressures in these zones. The process of dividing into zones continues until the main zone becomes less than 1-2% of the current volume of the cylinder.

The calculation of detonation starts from the very beginning of the process, when combustion has not yet begun even in the zone of the oil jet. Based on the charge parameters in the main zone  $p$ ,  $T_{m.z}$ ,  $\alpha_{gas}$ ,  $BG_{Fm.z}$ , the Livengood-Wu integral (3) is calculated in order to assess the readiness of the mixture for self-ignition, which is then used to estimate the tendency to detonation. Such an approach to the calculation of detonation "Shellknockmodel" was proposed by Ricardo in 1997 [19] as applied to gasoline engines with spark ignition.



In this study of a dual-fuel diesel engine, the theoretical auto-ignition delay period  $\tau_{iT}$  in the main zone is determined at each computational step by calculating the detailed chemical kinetics of pre-flame reactions (in the CHEMKIN program). For hydrogen-air mixtures, the LLNL\_v1\_ab mechanism is used [25]. Due to the high detonation activity of a mixture of hydrogen and air, estimating the readiness of this mixture for detonation only by the value of the integral LW is inconvenient, since it can vary over a very wide range depending on the conditions during the combustion process. Therefore, we used the charge readiness for detonation indicator LWknock, which is defined as follows. If the gas-air mixture is poor, the compression ratio is low, then the integral LW in the main zone increases slowly and does not reach unity by the end of the fresh charge burnout. In this case, it is assumed that there are no conditions for detonation, combustion is knock-free, and LWknock = LWz. As the hydrogen-air mixture is enriched, the combustion rate and the tendency to detonation increase, while the value of the integral LW can reach unity until the end of hydrogen burnout in the main zone. The moment of reaching LW=1 in the scale of the relative duration of hydrogen burnout in the main zone is designated as  $\phi LWz$ . For the condition  $\phi LWz < 1$ , the detonation readiness indicator is calculated as: LWknock = 2 -  $\phi LWz$  (where  $\phi LWz$  is the relative duration of hydrogen burnout). Thus, the detonation readiness indicator describes the quantitative and qualitative propensity of the mixture in the cylinder to detonation: at LWknock < 1 detonation does not occur, at 1 < LWknock < 2 detonation occurs in the process of hydrogen combustion; at 2 < LWknock, detonation occurs even before combustion starts. The detonation model is identified by refining the coefficient kknock in formula (4), which is used to calculate the integral LW when simulating this process:

$$LW = \int_0^{\tau_i} \frac{d\tau}{k_{knock} \tau_{iT}}. \quad (4)$$

After analyzing the experimental data [22], it was accepted that  $k_{knock} = 1.7$ .

## 4 Computational studies of the working process of a dual-fuel hydrogen engine

In the work, the working process of the D-245 dual-fuel hydrogen engine operating at nominal mode was studied. At  $\varepsilon = 8$ , the engine develops power  $N_e = 63.8$  kW at  $n = 2200$  min<sup>-1</sup>. Some parameters of the operation of this engine are given in Table 5.

**Table 5.** Comparative parameters of the working process of diesel type D-245 (4 CHN 11/12.5) in full power mode with different proportions of hydrogen,  $\varepsilon = 8$ ,  $\theta = 14^\circ$  c.v. up to TDC.

Parameters	Mode number						
	No 1	No 2	No 3	No 4	No 5	No 6	No 7
Share of hydrogen, %	0	5	10	20	40	60	80
Effective power $N_e$ , kW	63.8	64.2	65.1	66.4	68.0	66.6	64.0
Total specific effective fuel consumption $g_e$ , g/(kWh)	275.0	270.7	266.8	261.9	255.7	261.1	271.5
Effective efficiency	0.308	0.311	0.316	0.322	0.330	0.323	0.311
Excess air coefficient $\alpha$	2.020	2.027	2.024	2.017	2.010	2.009	2.012
Excess air coefficient for gas $\alpha_{gas}$ (excluding oil diesel fuel)	-	48.8	24.2	11.9	5.72	3.69	2.68
Maximum combustion pressure $p_z$ , bar	40.3	41.0	42.0	44.8	51.7	56.6	61.1
Maximum combustion temperature $T_{max}$ , K	1518	1535	1570	1618	1753	1868	1997

Average diameter of drops according to Sauter $d_{32}$ , $\mu\text{m}$	35.0	35.3	35.7	36.2	37.6	41.2	48.1
$LW_{knock}$ readiness indicator for detonation	0.075	0.137	0.218	0.398	0.702	1.070	1.307
Specific carbon dioxide emission $e_{CO_2}$ , g/(kWh)	888	832	777	678	496	338	176
Exhaust gas concentration of nitrogen oxides $C_{NO_x}$ , ppm	832	860	891	932	1060	1170	1300
Exhaust smoke $K_X$ , % on the Hartridge scale	15.0	13.5	12.5	10.5	7.0	4.5	3.0

After optimizing the values of the compression ratio  $\varepsilon$  and the injection advance angle of the ignition diesel fuel  $\theta$ , the following was chosen:  $\varepsilon = 8$  and  $\theta = 5^\circ$  p.c.v. to TDC. Comparative parameters of the working process of diesel type D-245 (4 CHN 11/12.5) in full power mode with different additives of hydrogen are presented in Table 5.

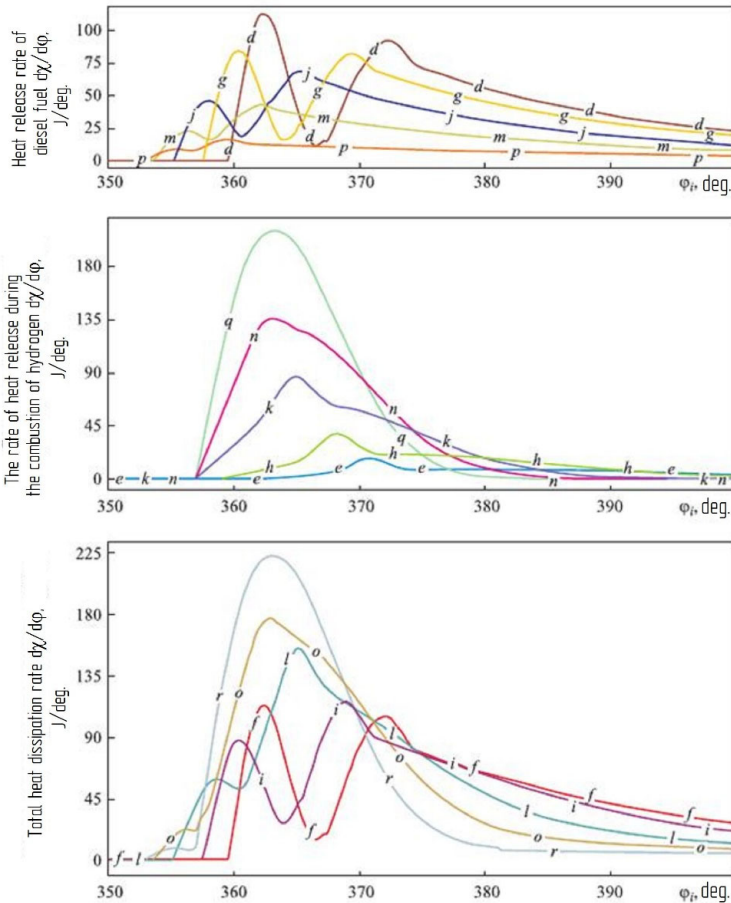


**Fig. 5.** Evolution of the rate of heat release from the combustion of diesel fuel, from the combustion of hydrogen and total heat release as the hydrogen content in the cycle portion in a diesel engine of the D-245 type (4 CHN 11/12.5) in full power mode  $\varepsilon = 8$ , advancing the injection of diesel fuel  $\theta = 5^\circ$  PKV to TDC; proportion of hydrogen:  $d - 10\%$ ;  $g - 20\%$ ;  $j - 40\%$ ;  $m - 60\%$ ;  $p - 80\%$ ;  $e - 10\%$  ( $\alpha_{gas}=23,3$ );  $h - 20\%$  ( $\alpha_{gas}=11,5$ );  $k - 40\%$  ( $\alpha_{gas}=5,55$ );  $n - 60\%$  ( $\alpha_{gas}=3,60$ );  $q - 80\%$  ( $\alpha_{gas}=2,62$ );  $f - 10\%$ ;  $i - 20\%$ ;  $l - 40\%$ ;  $o - 60\%$ ;  $r - 80\%$ ;  $\alpha_{gas}$  – excess air coefficient for gas.

Figure 5 shows the evolution of the rates of heat release from the combustion of diesel fuel and from the combustion of hydrogen, as well as the total heat release as the hydrogen content in the total fuel supply in the D-245 diesel engine increases. At a low supply of H<sub>2</sub>, the heat release rate has a clear tendency to a shape with two pronounced peaks. They are due to the low degree of compression and, as a result, a long delay period for self-ignition of diesel fuel (approximately 20 ° c.c.v.). With a long delay in self-ignition, almost 24% of diesel fuel has time to evaporate and burns out according to the volumetric mechanism. A depleted mixture of hydrogen and air burns relatively slowly and its contribution to the total heat release is insignificant and extended over time. In modes with a high hydrogen content, combustion is determined by a rapidly burning hydrogen-air mixture. Diesel fuel, on the other hand, burns for a relatively long time due to the large diameter of the droplets that form as a result of a short injection of a small portion of diesel fuel. To overcome the negative impact of lowering the compression ratio on fuel economy, it is necessary to influence the operating process in order to reduce the severity of the combustion process.

The generalized calculation data for the D-245 diesel engine operating at full power on an oil diesel engine and with hydrogen supply to the CS indicate that the maximum value of the effective efficiency of the diesel engine under study  $\eta_e=33.0\%$  corresponds to the supply of 40% hydrogen to the CC (Table 5). In this case, compared to operation only on oil diesel fuel ( $\eta_e=30.8\%$ ), the effective efficiency  $\eta_e$  increased by 7%. With a further increase in the amount of hydrogen supplied to the CC, the values of the effective efficiency decrease. But with an increase in the amount of hydrogen supplied to the combustion chamber, a significant increase in the maximum combustion pressure  $p_z$  (from 40.3 to 61.1 bar) and the maximum combustion temperature  $T_{max}$  (from 1245 to 1724 °C) was noted. As noted above, it is convenient to use the  $LW_{knock}$  parameter as an indicator characterizing the tendency of the mixture to knock. If this parameter  $LW_{knock} < 1$ , then knocking does not occur. Among the studied modes, only two modes - with hydrogen supply of 60 and 80% have the parameter  $LW_{knock} > 1$  (1.070 and 1.307, respectively, see Table 5), which indicates detonation combustion in these modes [26]. From the point of view of fuel efficiency and indicators of the dynamics of the combustion process, the regime with a hydrogen supply of 40% should be considered optimal, in which the effective efficiency of the diesel engine is maximum  $\eta_e=33.0\%$ , and the parameter  $LW_{knock} = 0.702$ . The transfer of a diesel engine from oil diesel fuel to work with the addition of hydrogen in an amount of 40% is accompanied by a decrease in the specific emission of carbon dioxide  $e_{CO_2}$  from 888 to 496 g/(kWh), i.e. by 44%. At the same time, the opacity of the exhaust gas  $K_X$  decreased from 15.0 to 7.0% on the Hartridge scale, i.e. by 53% [27]. However, in this case, the content of nitrogen oxides  $C_{NOx}$  in the exhaust gas increases from 832 to 1060 ppm, i.e. by 27%.

## 5 Conclusion

The research results can be summarized in the following main conclusions:

1. When studying the working process of the dual-fuel hydrogen engine D-245, hydrogen was ignited from the ignition dose of diesel fuel. In this case, hydrogen was supplied to the diesel intake system, and diesel fuel was injected with a standard fuel supply system. To reduce the rigidity of the combustion of the working mixture, the compression ratio was reduced from 15 to 8, FIAA was reduced from 14 to 5° c.v. to TDC, the diesel engine was derated in terms of rotational speed from 2400 to 2200 min<sup>-1</sup>. The share of hydrogen in the total fuel supply was 5, 10, 20, 40, 60, and 80% (taking into account the difference in the combustion heat of diesel fuel and hydrogen).
2. From the point of view of fuel efficiency and indicators of the dynamics of the combustion process, the regime with the supply of hydrogen equal to 40% should

be considered optimal, in which the effective efficiency of the diesel engine is maximum and equal to 33.0%. In this case, compared to running on diesel oil alone, the effective efficiency  $\eta_e$  increased by 7%. At the same time, the forced decrease in the compression ratio to  $\varepsilon = 8$  leads to the fact that the effective efficiency of a gas diesel engine with hydrogen supply is lower than when implementing a diesel cycle.

3. The transfer of a diesel engine from oil-fired diesel fuel to operation with a hydrogen addition of 40% was accompanied by a decrease in carbon dioxide emissions  $e_{CO_2}$  from 888 to 496 g/(kWh), i.e. by 44%. At the same time, the opacity of the exhaust gas KX decreased from 15.0 to 7.0% on the Hartridge scale, i.e. by 53%. But there was an increase in the content of nitrogen oxides  $C_{NO_x}$  in the exhaust gas from 832 to 1060 ppm, i.e. by 27%.

## References

1. E. I. Zoulias, N. Lymberopoulos, *Hydrogen-Based Autonomous Power Systems: Techno-Economic Analysis of the Integration of Hydrogen in Autonomous Power Systems* (Springer, 2008)
2. C. M. White, R. R. Steeper, A. E. Lutz, *International Journal of Hydrogen Energy* **31(10)**, 1292-1305 (2006)
3. P. Dimitriou, T. Tsujimura, *International Journal of Hydrogen Energy* **42**, 24470-24486 (2017)
4. C. M. White, R. R. Steeper, A. E. Lutz, *International Journal of Hydrogen Energy* **31**, 1292-1305 (2006)
5. M. G. Shirk et al, *International Journal Hydrogen Energy* **33(23)**, 7237-7244 (2008)
6. S. Szwaja, K. G. Rogalinski, *International Journal Hydrogen Energy* **34(10)**, 4413-4421 (2009)
7. S. Verhelst, T. Wallner, *Progress in Energy and Combustion Science* **35(6)**, 490-527 (2009)
8. K. J. Lee et al, *International Journal of Hydrogen Energy* **38**, 255-264 (2013)
9. W. B. Santoso, R. A. Bakar, A. Nur, *Energy Procedia* **32**, 3-10 (2013)
10. P. A. Caton, J. T. Pruitt, *International Journal of Engine Research* **10**, 45-63 (2009)
11. C. Liew et al, *Fuel* **91**, 155-163 (2012)
12. M. N. Taxon, S. R. Brueckner, S. V. Bohac, *SAE Technical Paper Series* **2002-01-2685**, 1-20 (2002)
13. Liu et al, *International Journal of Hydrogen Energy* **46**, 1302-1314 (2020)
14. T. Sandalci, Y. Karagöz, *International Journal of Hydrogen Energy* **39**, 18480-18489 (2014)
15. P. Selvi Rajaram, A. Kandasamy, P. Arokiasamy Remigious, *Thermal Science* **18(1)**, 259-268 (2014)
16. E. Tomita et al, *SAE Technical Paper Series* **2001-01-3503**, 1-10 (2001)
17. V. A. Chintala, K. A. Subramanian, *Renewable and Sustainable Energy Reviews* **70**, 472-491 (2017)
18. N. Saravanan, G. Nagarajan, *Applied Energy* **87(7)**, 2218-2229 (2010)
19. A. S. Kuleshov, *SAE Technical Paper Series* **2005-01-2119**, 1-10 (2005)
20. A. S. Kuleshov, *SAE Technical Paper Series* **2007-01-1908**, 1-10 (2007)

21. A. Kuleshov, L. Grekhov, SAE Technical Paper Series **2013-01-0882**, 1-16 (2016)
22. M. Mehl et al, Proceedings of the Combustion Institute **33**, 193-200 (2011)
23. A. S. Kuleshov, SAE Technical Paper Series **2009-01-1956**, 1-21 (2009)
24. C. D. Rakopolous et al, International Journal of Hydrogen Energy **36**, 5163-5180 (2011)
25. D. T. Koch et al, SAE Technical Paper Series **2019-01-2178**, 1-11 (2019)
26. R. Heindl et al, SAE Technical Paper Series **2009-01-1421**, 1-20 (2009)
27. M. O. Connaire et al, International Journal of Chemical Kinetics **36**, 603-622 (2004)